# On the pathways and timescales of intercontinental air pollution transport

Andreas Stohl, Sabine Eckhardt, Caroline Forster, Paul James, and Nicole Spichtinger
Lehrstuhl für Bioklimatologie und Immissionsforschung, Technical University of Munich, Freising, Germany

Received 15 October 2001; revised 5 April 2002; accepted 8 April 2002; published 4 December 2002.

[1] This paper presents results of a 1-year simulation of the transport of six passive tracers, released over the continents according to an emission inventory for carbon monoxide (CO). Lagrangian concepts are introduced to derive age spectra of the tracer concentrations on a global grid in order to determine the timescales and pathways of pollution export from the continents. Calculating these age spectra is equivalent to simulating many (quasi continuous) plumes, each starting at a different time, which are subsequently merged. Movies of the tracer dispersion have been made available on an Internet website. It is found that emissions from Asia experience the fastest vertical transport, whereas European emissions have the strongest tendency to remain in the lower troposphere. European emissions are transported primarily into the Arctic and appear to be the major contributor to the Arctic haze problem. Tracers from an upwind continent first arrive over a receptor continent in the upper troposphere, typically after some 4 days. Only later foreign tracers also arrive in the lower troposphere. Assuming a 2-day lifetime, the domestic tracers dominate total tracer columns over all continents except over Australia where foreign tracers account for 20% of the tracer mass. In contrast, for a 20-day lifetime even continents with high domestic emissions receive more than half of their tracer burden from foreign continents. Three special regions were identified where tracers are transported to, and tracer dilution is slow. Future field studies therefore should be deployed in the following regions: (1) In the winter, the Asia tracer accumulates over Indonesia and the Indian Ocean, a region speculated to be a stratospheric fountain. (2) In the summer, the highest concentrations of the Asia tracer are found in the Middle East. (3) In the summer, the highest concentrations of the North America tracer are found in the Mediterranean. *INDEX TERMS:* 0322 Atmospheric Composition and Structure: Constituent sources and sinks; 0368 Atmospheric Composition and Structure: Troposphere—constituent transport and chemistry; 3309 Meteorology and Atmospheric Dynamics: Climatology (1620); 3364 Meteorology and Atmospheric Dynamics: Synoptic-scale meteorology

**Citation:** Stohl, A., S. Eckhardt, C. Forster, P. James, and N. Spichtinger, On the pathways and timescales of intercontinental air pollution transport, *J. Geophys. Res.*, *107*(D23), 4684, doi:10.1029/2001JD001396, 2002.

## 1. Introduction

[2] Atmospheric transport of trace substances involves many space- and timescales. Intercontinental transport (ICT) occurs on timescales on the order of 3–30 days and is thus most relevant for substances having a lifetime within this range. This involves such different species as ozone ($O_3$) and its precursors, aerosols, mercury, and persistent organic pollutants. ICT also influences shorter- (e.g., radicals) and longer-lived species (e.g., most of the greenhouse gases) through chemical reactions with the intermediate-lived compounds.

[3] With measurement techniques, particularly remote sensing, becoming suitable for the purpose of studying ICT during the past few years, evidence of its occurrence has accumulated. Furthermore, atmospheric transport models are now capable of establishing source-receptor relationships over such long distances. However, many studies still fail to link observations unambiguously to ICT, and individual reports have not yet been distilled into a coherent picture. This study aims at characterizing the timescales and the pathways of ICT, both to put past observations into perspective, and to provide guidance on where and when future field campaigns should be deployed to study ICT most effectively. The paper is organized such that we present a review of ICT observations in section 2, describe our methods in section 3, discuss general transport characteristics in section 4, quantify ICT in section 5, and finally draw conclusions in section 6.


0148-0227/02/2001JD001396$09.00

## 2. Review

### 2.1. Africa

[4] Sometimes Saharan dust can be transported both to northeastern South America (during winter) and into the Caribbean (during summer) with the trade winds [*Swap et*

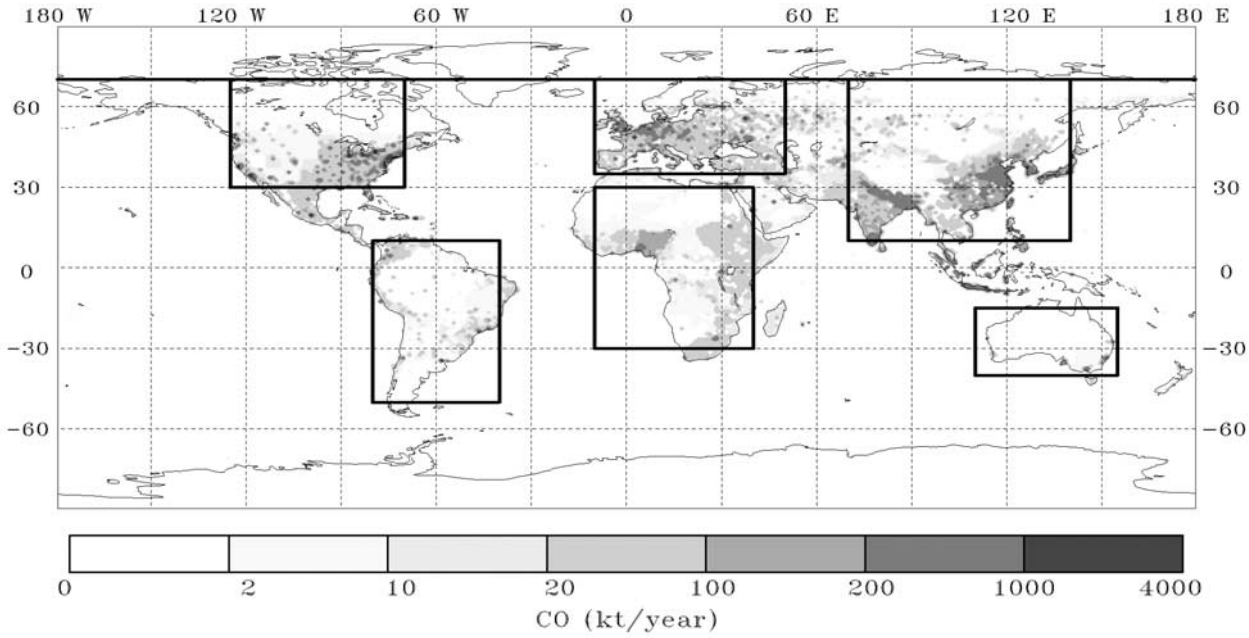


**Figure 1.** Anthropogenic CO emissions in kilotons CO per year according to the EDGAR inventory. The rectangles mark the continental boxes used for evaluating ICT in section 4.

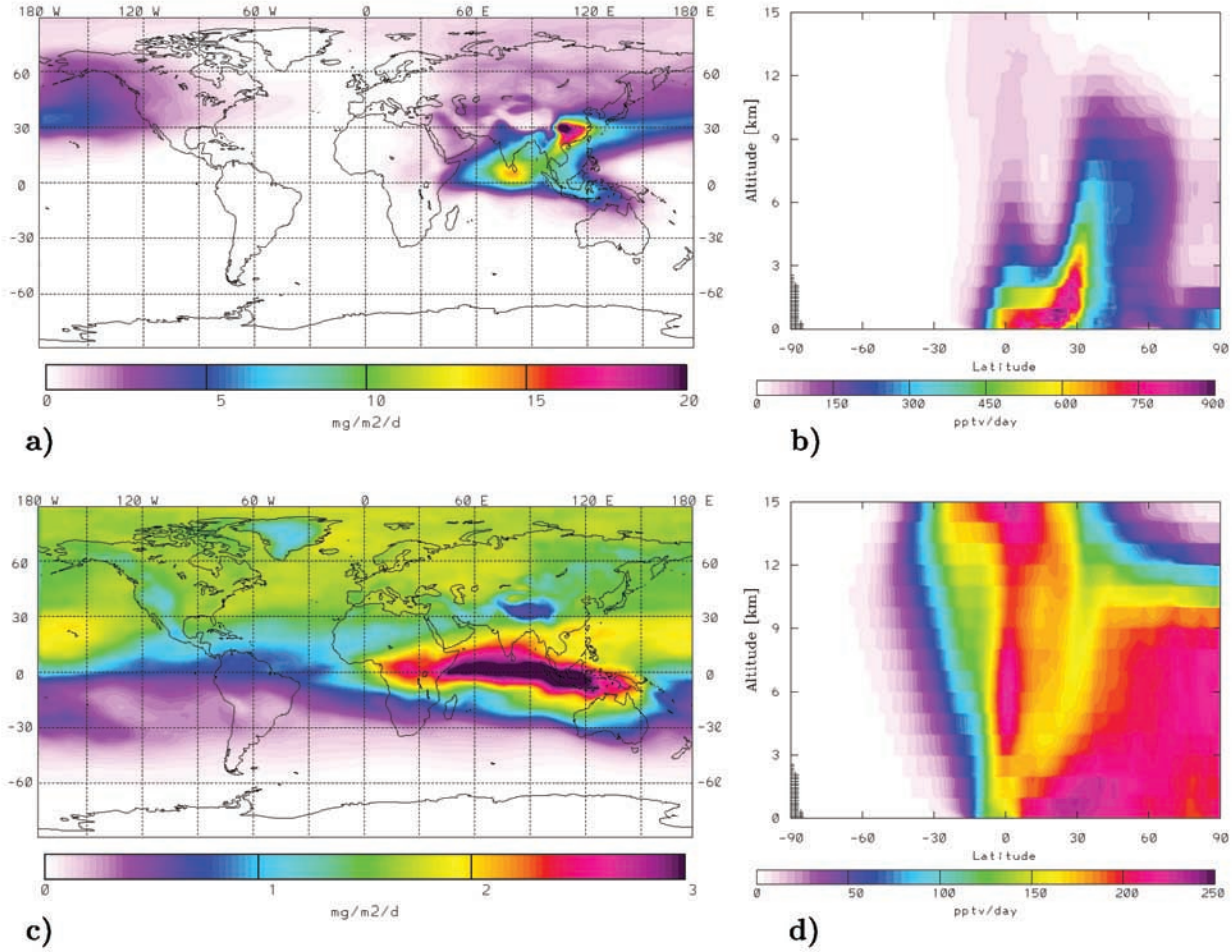


**Figure 2.** Total columns (a, c) and zonally averaged mixing ratios (b, d), both divided by the respective time interval, of the Asia tracer for ages of 6–8 days (a, b) and 25–30 days (c, d) during DJF.

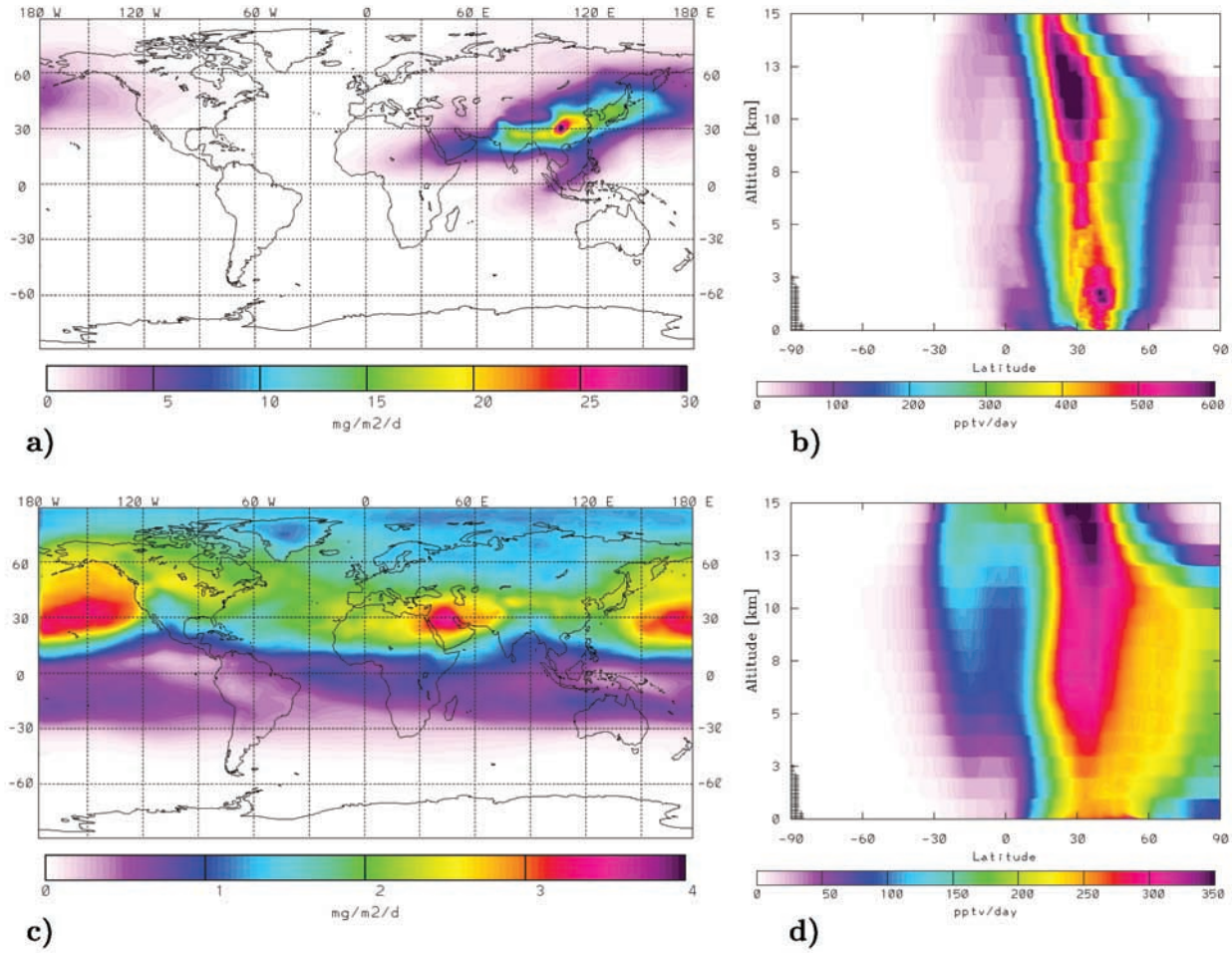


**Figure 3.** Same as Figure 2, but for JJA.

*al.*, 1996; *Prospero*, 1999]. Dust transports into the Mediterranean are also very common, and sometimes the dust can even reach northwestern Europe [*Reiff et al.*, 1986]. $O_3$ formed in African biomass burning plumes can be exported both to the tropical Atlantic [*Fishman et al.*, 1991] and to the Pacific, depending on the fire location and season. Nitrogen oxides and sulfur dioxide emitted by power plants in South Africa can travel all the way to Australia if they get entrained into the midlatitude stormtrack after a period of local accumulation in the subtropical high [*Wenig et al.*, 2002]. South African emissions can also be transported offshore and then back to the continent in the flow around the subtropical high [*Garstang et al.*, 1996; *Tyson and D'Abreton*, 1998]. Such recirculations also occur at other places, particularly in the subtropics, and can easily be confused with ICT because trace gas signatures in the recirculating air mass may be indistinguishable from those of ICT.

### 2.2. Asia

[5] Export pathways from Asia fluctuate strongly with season, as the location and strength of the Japan jet varies with the position of the subtropical Pacific high. Dust from Asia is observed quite frequently at the Mauna Loa observatory on Hawaii. During April 1998 an exceptional trans-Pacific transport event of dust from the Gobi desert caused increases in particulate matter concentrations in North America, even at the surface [*Wilkening et al.*, 2000; *Husar et al.*, 2001]. Observations of elevated concentrations of many different species over North America were traced to an Asian source, including organochlorine pesticides [*Bailey et al.*, 2000], sulfate [*Andreae et al.*, 1988], CO and peroxyacetyl nitrate in northwestern North America [*Jaffe et al.*, 1999], and photochemical air pollution over California [*Parrish et al.*, 1992]. Model studies suggest that Asian emissions could be important for pollutant concentrations over North America in the future if they continue to grow [*Berntsen et al.*, 1999; *Jacob et al.*, 1999]. Transport at high altitudes is an important element of ICT. In a model study *Yienger et al.* [2000] found that Asian emissions had the maximum impact on CO over North America in the upper troposphere. *Wild and Akimoto* [2001], in another model study, found that Asian emissions are more efficient in producing $O_3$ than European and North American sources, and thus have the greatest influence on $O_3$ over other continents. Again the largest influence was found in the upper troposphere.

### 2.3. Australia

[6] There is little evidence of pollution export from Australia, but *Sturman et al.* [1997] reviewed papers on

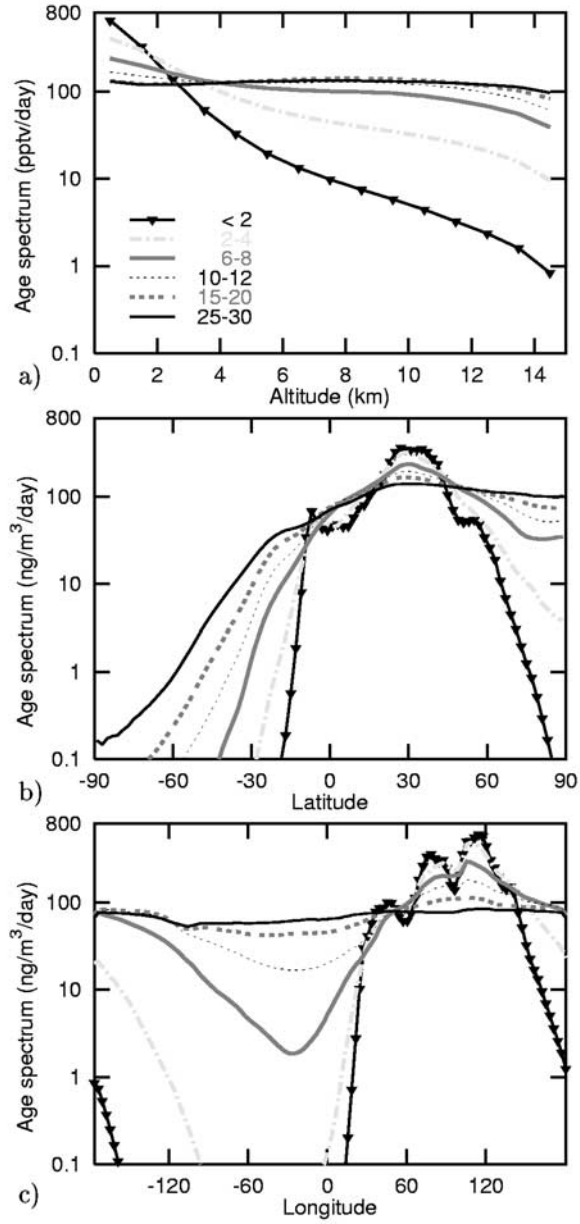


**Figure 4.** Annually averaged transport characteristics of the Asia tracer: a) vertical distribution of the horizontally averaged tracer mixing ratio, b) meridional distribution of the zonally and vertically averaged tracer concentration, and c) zonal distribution of the meridionally and vertically averaged tracer concentrations. Results for six age classes are drawn. The legend is placed in the top panel only.

insect and dust transport from Australia to New Zealand. They found that transport of air from Southern Australia to New Zealand occurs both in summer and in winter.

### 2.4. Europe

[7] *Newell and Evans* [2000] estimated that some 25% of the air parcels arriving over Central Asia have crossed over Europe before and some 4% have originated in the European boundary layer. But because of a lack of measurement data, there is little experimental evidence of European pollution export to Asia. Measurements of lead isotopes at Barbados during the 1970s and 1980s suggest that a major fraction of the lead originated from Europe, was transported southwards to Africa and then westward with the trade winds [*Hamelin et al.*, 1989]. A model study suggests that under special meteorological conditions, $O_3$ produced from European emissions can also be transported westward to North America within the midlatitudes [*Li et al.*, 2001a]. However, due to Europe's location at high latitudes its pollution can be transported toward the Arctic, contributing to what has become known as the Arctic haze [*Barrie*, 1986]. Due to high static stability, low temperatures and lack of solar radiation in winter, residence times of many compounds are longer there than anywhere else, leading to accumulation of pollutants north of the arctic front. It has been suggested that the major pathways delivering this pollution to the Arctic are from Eurasia [*Barrie*, 1986; *Jaeschke et al.*, 1999]. This is also important for the high concentrations of mercury [*Lu et al.*, 2001] and persistent organic pollutants in arctic snow.

### 2.5. North America

[8] *Parrish et al.* [1998] reported a clear influence of North American sources on $O_3$ and CO at 1 km above sea level at the Azores in the central North Atlantic. Hints on pollution transport from North America were found at Izaña on Tenerife [*Schmitt*, 1994] and at Mace Head, Ireland [*Jennings et al.*, 1996], but these episodes are infrequent and corresponding $O_3$ enhancements are marginal [*Derwent et al.*, 1998]. Transport of emissions from boreal forest fires in Canada caused a dense haze layer over Germany in August 1998 [*Forster et al.*, 2001]. $O_3$ concentrations were enhanced, too, and CO variations at Mace Head were dominated by this source over a one-month period. $NO_x$ was also emitted and transported across the Atlantic [*Spichtinger et al.*, 2001]. Model studies by *Wild et al.* [1996] and *Schultz et al.* [1998] showed that the key factor favoring $O_3$ transport from North America to Europe is lifting of the polluted air to higher altitudes, as transport is faster there and chemical lifetimes of $O_3$ and its precursors are longer. *Stohl and Trickl* [1999] presented a case study of high $O_3$ concentrations produced over North America that were transported within a warm conveyor belt (WCB), a warm moist airstream ahead of a cold front, to the upper troposphere over Europe. *Stohl* [2001] showed that WCBs often draw their inflow from the Asian and North American seaboards and can thus subject boundary layer air pollution from these continents to transport with the jet stream. Observations of trans-Atlantic transport have been reviewed by *Stohl and Trickl* [2001].

### 2.6. South America

[9] There is little evidence for export of South American pollution to other continents. *Thompson et al.* [1996] suggested that a significant fraction of the $O_3$ observed over Africa was produced in biomass burning plumes from South America.

## 3. Methods

[10] This study presents a 1-year simulation of the transport of anthropogenic emission tracers in order to identify

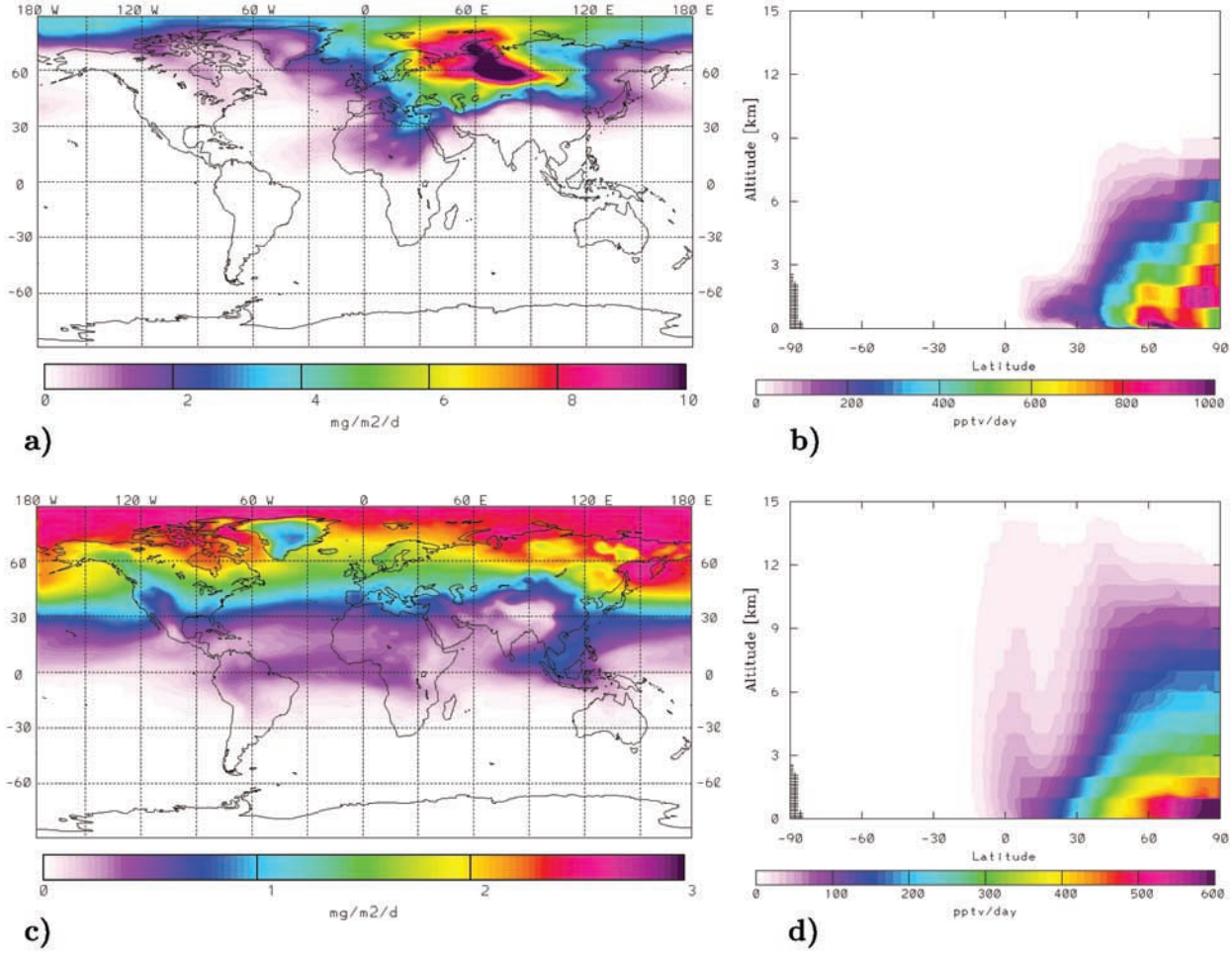


**Figure 5.** Same as Figure 2, but for the European tracer.

the pathways of pollution originating from the different continents over timescales up to 30 days after emission. Tracer transport was simulated with the Lagrangian particle dispersion model FLEXPART (version 4.0) [*Stohl et al.*, 1998; *Stohl and Thomson*, 1999] for the period January 2000 to February 2001. Only passive tracers are considered, which do not undergo chemical reactions or deposition processes. Documentation and the source code of FLEXPART can be obtained via the Internet from the address http://www.forst.tu-muenchen.de/EXT/LST/METEO/stohl/. FLEXPART was validated with data from three large-scale tracer experiments in North America and Europe [*Stohl et al.*, 1998]. FLEXPART was also used previously in several case studies of ICT [*Stohl and Trickl*, 1999; *Forster et al.*, 2001; *Spichtinger et al.*, 2001; *Wenig et al.*, 2002] and captured these events, and also intrusions of stratospheric air filaments into the lower troposphere [*Stohl et al.*, 2000], with high accuracy. Therefore, model validation is not a subject of this paper. We want to point out, though, that due to its Lagrangian nature, FLEXPART can preserve very fine-scale structures, as they are typically generated during ICT events. This puts it at an advantage over Eulerian transport models which suffer from numerical diffusion that tends to disperse these filaments.

[11] FLEXPART is driven with model-level data from the European Centre for Medium-Range Weather Forecasts [*ECMWF*, 1995] with a horizontal resolution of 1°, 60 vertical levels and a time resolution of 3 h (analyses at 0, 6, 12, 18 UTC; 3-h forecasts at 3, 9, 15, 21 UTC). FLEXPART treats advection and turbulent diffusion by calculating the trajectories of a multitude of particles. Stochastic fluctuations, obtained by solving Langevin equations [*Stohl and Thomson*, 1999], are superimposed on the grid-scale winds to represent transport by turbulent eddies.

[12] ECMWF data reproduce the large-scale effects of convection (e.g., strong ascent at the intertropical convergence zone (ITCZ) or within WCBs), but smaller-scale convective cells are not resolved. FLEXPART therefore was recently equipped with the convection scheme of *Emanuel and Zivkovic-Rothman* [1999]. This scheme is based on the grid-scale temperature and humidity data and provides a uniform treatment of all types (i.e., shallow to deep) of moist convection. A displacement matrix is calculated for every model column from which displacement probabilities for individual particles are derived. The scheme was tuned such that it best reproduces the convective precipitation fields that are generated on-line by the ECMWF model, in order to be as consistent as possible with

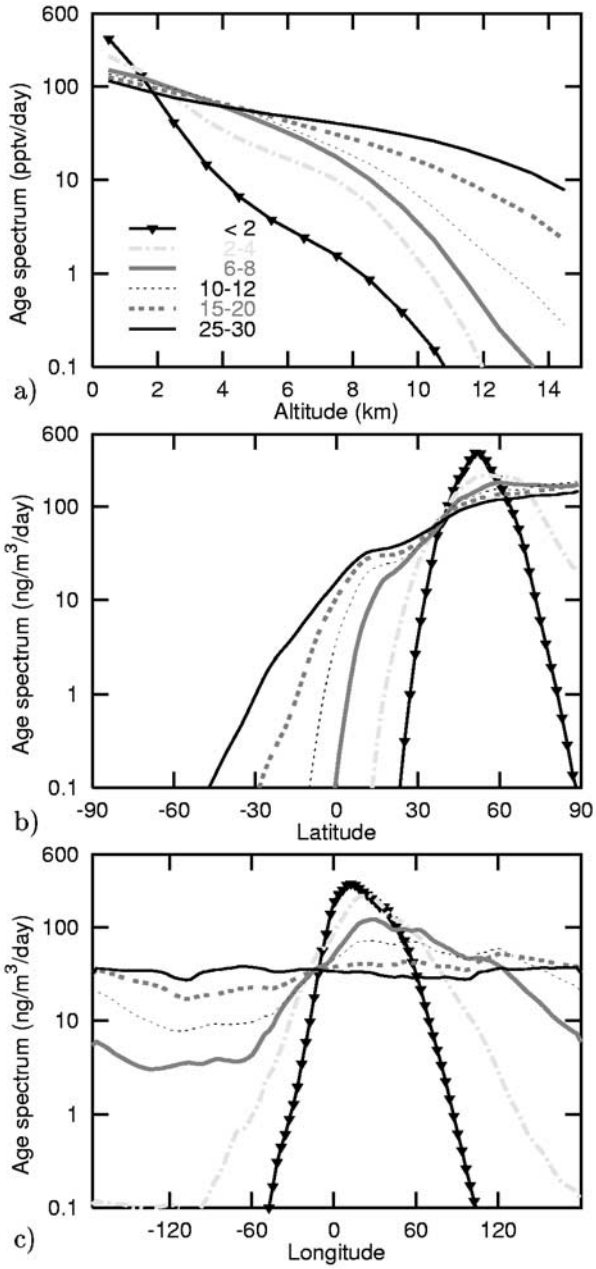


**Figure 6.** Same as Figure 4, but for the Europe tracer.

the driving meteorological model. A description of the implementation and some validation was presented by *Seibert et al.* [2001]. The overall effect of convection on the FLEXPART results is moderate, except for the tropics where it is important. Transport in the tropics is generally thought to be much less accurate than in the middle latitudes, both because of the strong convective activity and because fewer observations are available for the data assimilation at ECMWF than in the extratropics. We have made FLEXPART simulations with convection both turned on and turned off. Although there were some differences notable between these two model runs in the tropics (without convection the lifting into the upper troposphere was less pronounced), generally differences between these two simulations were very small (virtually everywhere concentration differences were less than 20%). This confirms our experience that much of the convection (especially slantwise convection in extratropical frontal systems, and convection in mesoscale convective complexes) is actually resolved in recent ECMWF analyses.

[13] Tracer mixing ratios and concentrations are determined on a three-dimensional grid (2° latitude × 3° longitude resolution and 15 layers up to 15 km) applying a kernel method. The transport of six continental pollution tracers was simulated, representing anthropogenic emissions taken from the EDGAR inventory [*Olivier et al.*, 1996] for CO for the base year 1990 (Figure 1). Africa, Asia, Australia, Europe, North America, and South Amer-

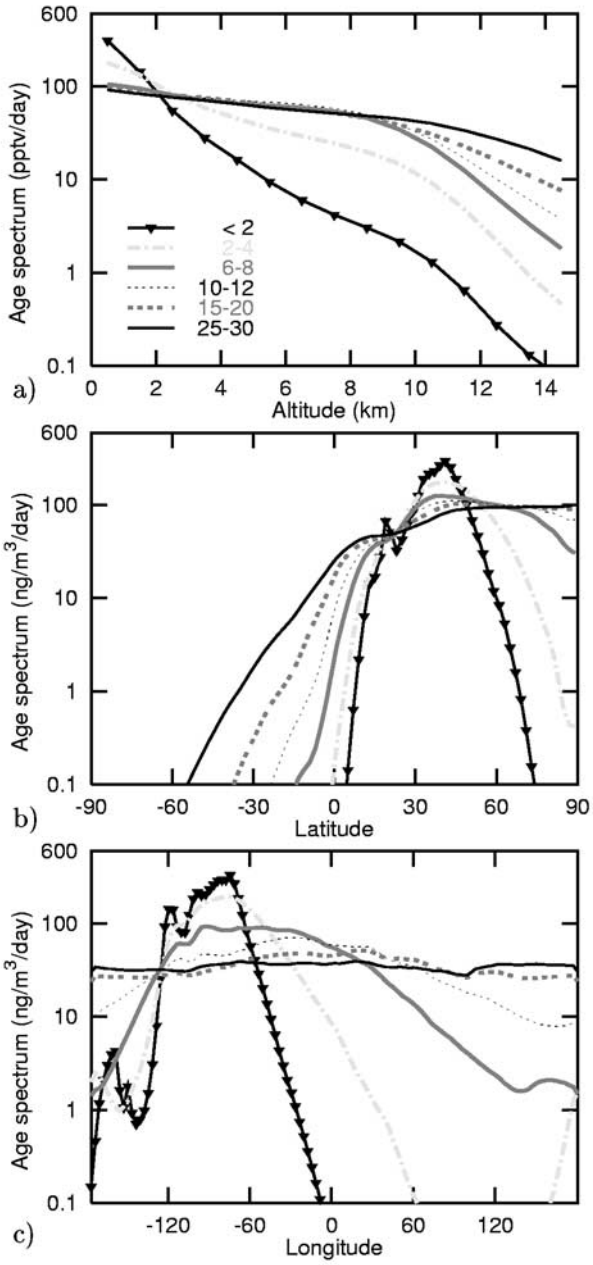


**Figure 7.** Same as Figure 4, but for the North America tracer.

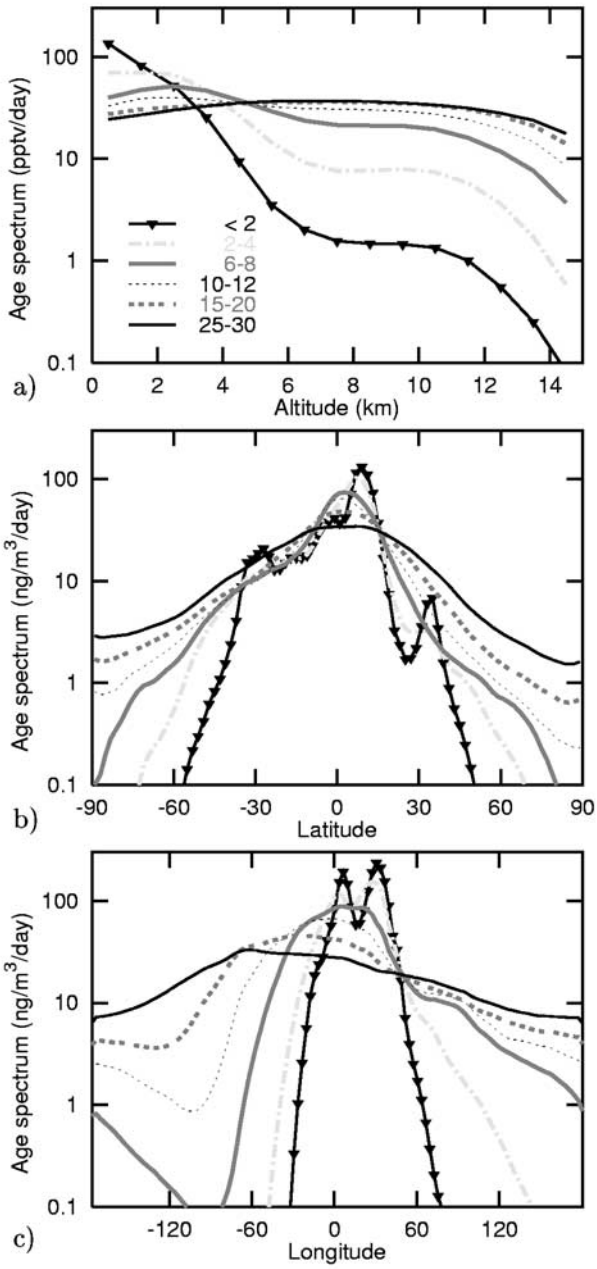


**Figure 8.** Same as Figure 4, but for the Africa tracer.

ica contribute approximately 11%, 43%, 1%, 20%, 21% and 5%, respectively, to the global anthropogenic CO emissions. Emissions are highest at the east coasts of Asia and North America, in India and Java, and in central and western Europe. In the southern hemisphere (SH), the highest emissions are found in South Africa. Since the emission patterns of many other compounds are similar to those of CO, and the focus here is on transport and not on chemistry, the CO tracer serves as a proxy for anthropogenic emissions. 2 million particles are released between the surface and 200 m over Asia, Europe and North America together, and 1 million particles over Africa, Australia and South America together every month. For each hemisphere all particles carry an equal amount of mass, and release locations are chosen randomly within each $1^\circ \times 1^\circ$ grid cell of the inventory. Time intervals between particle releases are shorter for high-emission grid cells than for low-emission cells to account for the different source strengths. Biomass burning emissions are also very important, but they are highly episodic, occur during specific meteorological situations, and their effective release height depends on many factors. Lacking this detailed information, we do not consider them in this study. Other reasons for not including them are that biomass burning emissions are much less important for other species such as nitrogen oxides and emission ratios between different species are highly variable both in time and space.

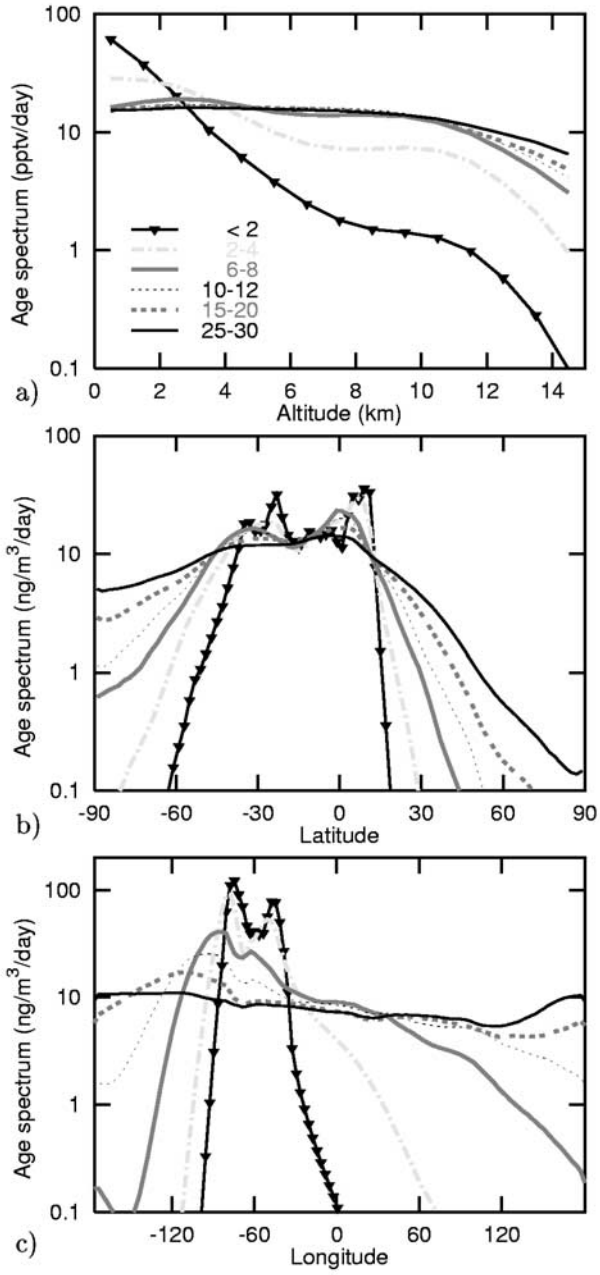


**Figure 9.** Same as Figure 4, but for the South America tracer.

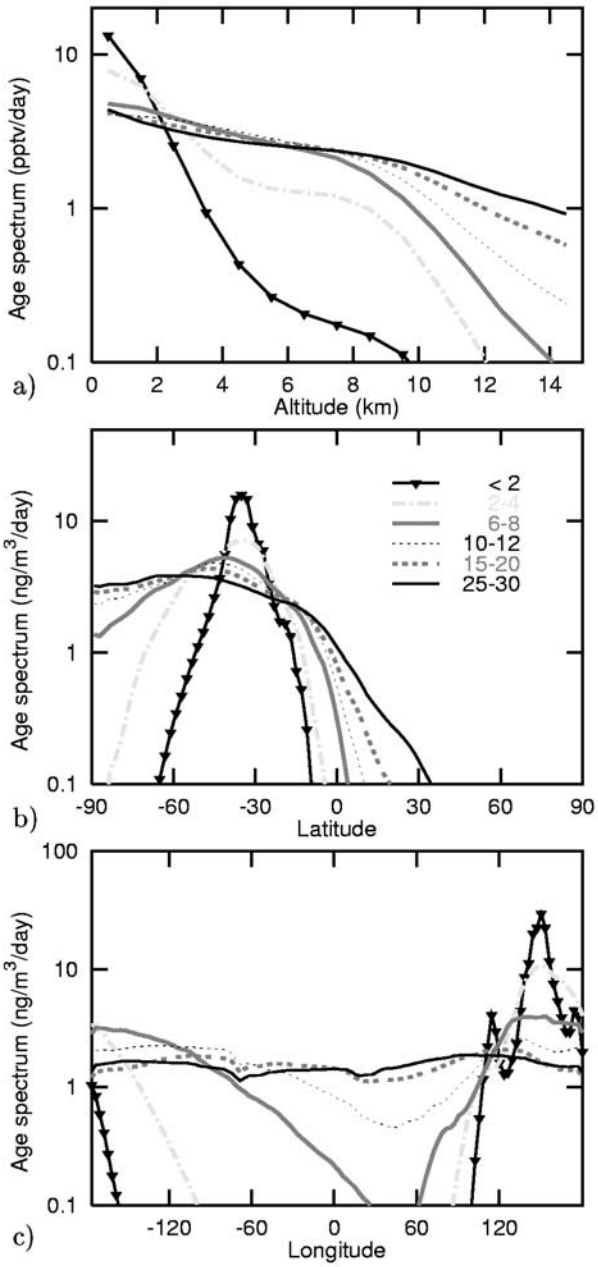


**Figure 10.** Same as Figure 4, but for the Australia tracer.

[14] Particles are tagged with their release time and are transported for 30 days. At every time step they are binned into 1 of 10 age classes (0–2, 2–4, 4–6, 6–8, 8–10, 10–12, 12–15, 15–20, 20–25, and 25–30 days, respectively), for each of which mixing ratios are calculated independently. Chemical or deposition processes are not considered. Note that deriving these age spectra is equivalent to simulating many individual (quasi continuous) plumes, each starting at a different time, which are subsequently merged. Seasonally averaged age spectra, as used in this study, thus are a superposition of all plumes occurring during that particular season. Because a spin-up time of 30 days is required, results are presented for a 1-year period beginning in February 2000, 1 month after the start of the simulation. In the following we present seasonal averages for March, April and May (MAM), June, July and August (JJA), September, October and November (SON), and December, January and February (DJF).

[15] The concept of the present study is different from the *Stohl* [2001] study, which identified where on Earth WCBs occur most frequently. These airstreams draw boundary layer air from the warm sector of low pressure systems and can transport this air into the upper troposphere on timescales of 1–2 days. The chemical characteristics of WCBs are discussed by *Cooper et al.* [2001], their most remarkable feature being washout of soluble species such as $HNO_3$ [*Stohl et al.*, 2002]. The main WCB inflow regions were found at the Asian and North American east coasts, relatively close to regions with high emissions. *Stohl* [2001] therefore speculated that emissions from Asia and North America, in contrast to those from Europe, are transported into the upper troposphere. However, no explicit link to emission transport could be made.

## 4. General Transport Characteristics

[16] As the largest differences occur between the pathways of the Asia tracer and the Europe tracer, we take these two as our first examples. Movies showing the dispersion of all six tracers, from which the following snapshots were taken, can be watched via the Internet at http://www.forst.tu-muenchen.de/EXT/LST/METEO/itct/itct.html.

[17] Figure 2 presents the distribution of the Asia tracer for age classes 4 (6–8 days) and 10 (25–30 days) in DJF. Horizontal distributions are shown as maps of the total CO tracer mass columns, divided by the time interval of the respective age class. Vertical distributions are shown as latitudinally averaged cross-sections of tracer mixing ratio (mixing ratios rather than concentrations are shown because in a well mixed state the mixing ratio is constant with height), divided by the time interval. Figure 2a shows that at 6–8 days, most of the tracer still remains relatively close to its source regions, an exception being tracer transported into the Pacific stormtrack at about 30° N. In fact, this portion of the emissions has spread almost throughout the entire North Pacific and some of it has already traveled to North America and beyond. The vertical cross-section (Figure 2b) shows that north of 30°N the height of the maximum mixing ratio is tilted toward higher latitudes, confirming that WCBs are mainly responsible [*Stohl*, 2001]. The small maximum at the surface close to the pole stems from emissions at high latitudes and has experienced transport similar to European emissions (see below). Tracer emitted south of about 30°N, and particularly in India, is on its way toward the ITCZ with the trade winds at 6–8 days. Note the important role of the winter monsoon circulation, recently explored by the INDOEX campaign [*Lelieveld et al.*, 2001]. Maximum mixing ratios are still found beneath the trade wind inversion, except for some of the tracer emitted in the southernmost parts of India that has arrived in the ITCZ and has reached high altitudes.

[18] At 25–30 days, tracer patterns in the midlatitude stormtrack differ considerably from those further south. North of 30°N, the tracer is mixed throughout the troposphere, both horizontally (Figure 2c) (the minima over mountain ranges are due to a lower depth of the atmosphere)

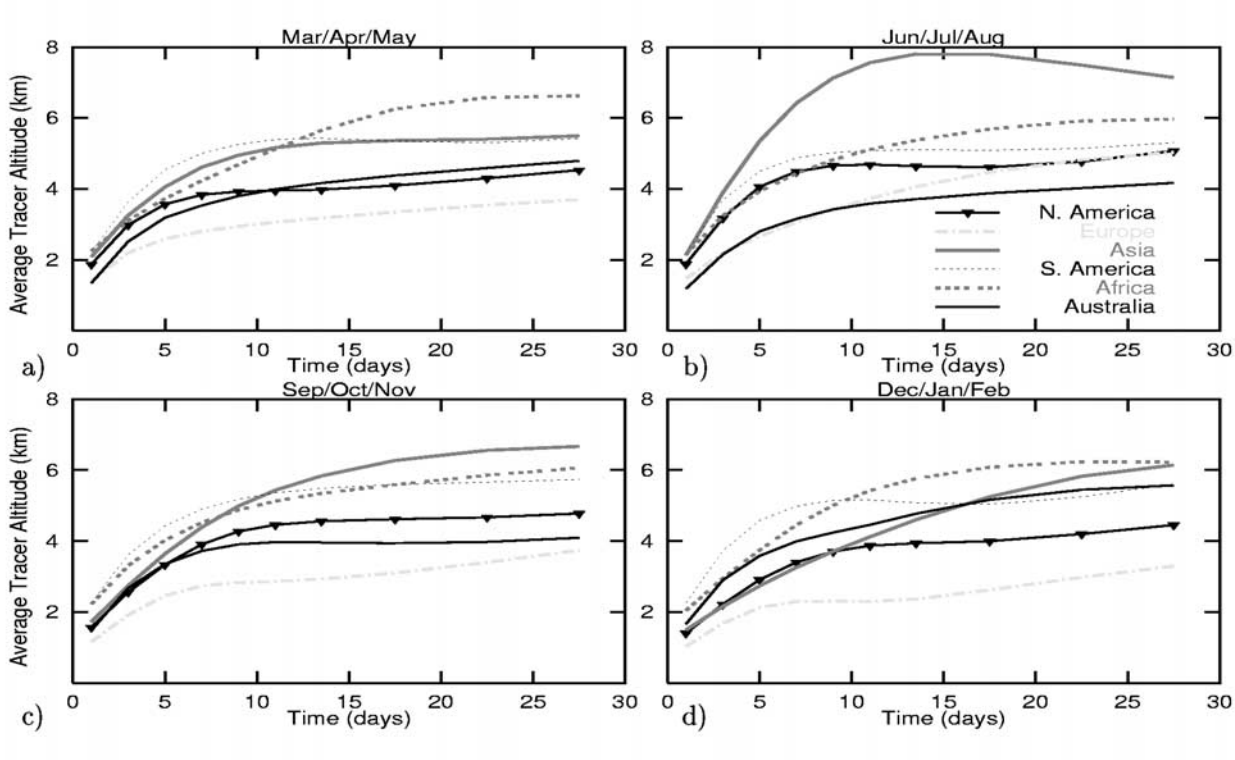


**Figure 11.** Average height in the atmosphere of the CO tracer mass in dependence of the tracer age, and for the four seasons, MAM (a), JJA (b), SON (c), and DJF (d), respectively. Shown are North America tracer (solid black line with triangles), Europe tracer (dash-dotted grey line), Asia tracer (thick dark grey line), South America tracer (dashed black line), Africa tracer (thick dotted grey line), and Australia tracer (solid black line), respectively.

and vertically (Figure 2d), bounded only by the tropopause at altitudes between approximately 9–12 km. In contrast, tracer south of 30°N still forms a compact plume within the tropical jet region over Indonesia and the equatorial Indian Ocean. Little mixing into the extratropical SH has occurred. Tracer in the equatorial maximum is found mostly in the middle and upper troposphere. Although our output (but not the computational) domain ends at 15 km, it is obvious that some of it is found at even higher altitudes and may have already entered the stratosphere. In fact, the Indonesia region is speculated to act as a stratospheric fountain [*Newell and Gould-Stewart*, 1981], where tropospheric air preferably enters the stratosphere. The fact that Asian emissions accumulate just in this region could have important implications, since substances that are long-lived enough and are not washed out finally reach the stratosphere.

[19] The situation is different in JJA (Figure 3). As the North Pacific stormtrack shifts southward, more tracer travels with the midlatitude westerlies, and less is transported toward the ITCZ (compare Figures 2a and 3a, but note the differences in the color scales). However, because of the weaker zonal circulation in summer, little tracer has reached the North American west coast at 6–8 days. Tracer from India, instead of tracking toward the equator as in DJF, now travels with the summer monsoon flow. Also the vertical tracer distribution is very different from the DJF situation (Figure 3b). The tracer mixing ratio maximizes at an altitude of about 12 km, a result of strong ascent in the monsoon flow. At midlatitudes, tracer is transported to higher altitudes, too.

[20] Differences to the DJF situation are even larger at 25–30 days. There are two strong maxima in the total tracer columns (Figure 3c), one over the subtropical Pacific, the other over the Middle East. The latter is due to a closed circulation over Southern Asia at 200 hPa in JJA [*Peixoto and Oort*, 1992], which transports tracer from South Asia westward after its ascent with the monsoon flow. The tracer then gets trapped in the subtropical anticyclone and slowly descends to lower levels. In a model simulation, *Li et al.* [2001b] have identified this region as the one with the highest $O_3$ concentrations worldwide in JJA, but this awaits confirmation from observations. The vertical tracer distribution (Figure 3d) shows maximum mixing ratios at the highest layer of our output grid, but less than 10% of the tracer mass resides above 15 km.

[21] Figure 4 summarizes the annual mean vertical (a), meridional (b) and zonal (c) distribution of the Asia tracer. Similar panels are shown below for the other tracers to facilitate comparisons. The mixing ratio maximizes at approximately 10 km for the age classes from 6 to 20 days, especially for summer conditions (not shown). This implies that Asia tracer is being pumped selectively into the upper troposphere, opposed to a diffusion-like dispersion process that would require counter-gradient fluxes to obtain higher mixing ratios in the upper than in the lower troposphere. Mixing and transport into the subtropical high-pressure

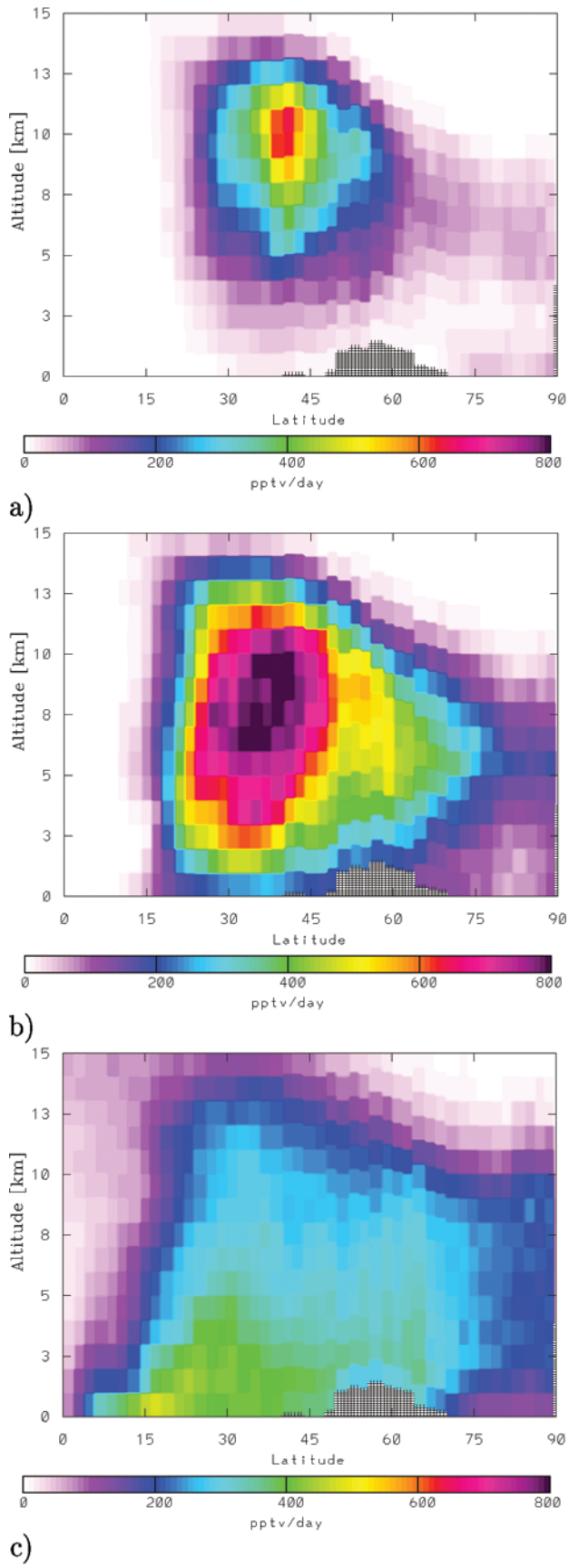


regions leads to a slow downward propagation of the tracer at later times.

[22] The Asia tracer experiences both the strongest vertical and meridional transport of all northern hemisphere (NH) continents. Transport into the SH is most pronounced in MAM and JJA, whereas transport toward the north pole peaks in DJF, giving an almost uniform tracer distribution between the equator and the north pole at 25–30 days. Zonal transport of the Asia tracer is the slowest of all NH tracers, because of its large portion traveling with the relatively slow tropical circulation.

[23] Europe tracer is emitted into an entirely different wind regime as the Asia tracer. Westerly winds prevail over Europe throughout the year as it is located at the highest latitudes of all continents. Cyclogenesis is less frequent than at the eastern seaboards of Asia and North America, because of Europe's location at the end (rather than the beginning) of the North Atlantic stormtrack. WCBs are thus also less frequent [*Stohl*, 2001], and those that do develop are shallower than their Asian and North American counterparts. Convection is also less vigorous over Europe, and therefore emissions from Europe tend to remain in the lower troposphere. This is most obvious in DJF when almost all of the Europe tracer tracks northeastward. At 6–8 days (Figure 5a), the plume center is located over northwestern Asia. A significant fraction has crossed the polar circle, and some of it has already reached Canada with easterly winds at polar latitudes. The vertical cross-section (Figure 5b) reveals that most of the tracer remains below 3 km, contrary to what was found for the Asia tracer (Figure 2b).

[24] At 25–30 days, the Europe tracer has accumulated north of the polar circle (Figure 5c). Due to subsidence in the polar high the Europe tracer descends in the Arctic, and thus the highest mixing ratios at the pole occur at the very lowest levels (Figure 5d). This highlights the severe impact European emissions appear to have for the Arctic haze problem. Despite its emissions being only half of the Asian ones, the Europe tracer at the lowest level at the pole is 3 times more abundant than the Asia tracer at 25–30 days. At earlier times the difference is even stronger.

[25] In summer (not shown), most of the Europe tracer is still advected toward the pole. However, it spreads more in the vertical and over a larger latitude range. At 25–30 days, a secondary plume exists over the Atlantic at about 15°N, clearly separated from the high tracer concentrations at latitudes north of about 50°N. This plume is due to some of the emissions, mostly from southern Europe, initially tracking across the Mediterranean and into Africa. Figure 6 shows the summary panel for the Europe tracer. Figure 6a confirms that vertical mixing is very slow (compare with the Asia tracer, Figure 4). Even at 25–30 days there is a strong vertical gradient during all seasons. Concentrations at the pole after 25–30 days are almost as high as over Europe for the first age class, indicating rather undiluted transport. Zonal transport is much faster than for the Asia tracer and mostly toward the east.

**Figure 12.** (opposite) Altitude-latitude sections of the Asia tracer at 125°W for ages of a) 4–6 days, b) 8–10 days, and c) 20–25 days, during MAM. The hatched area indicates the height of the topography.

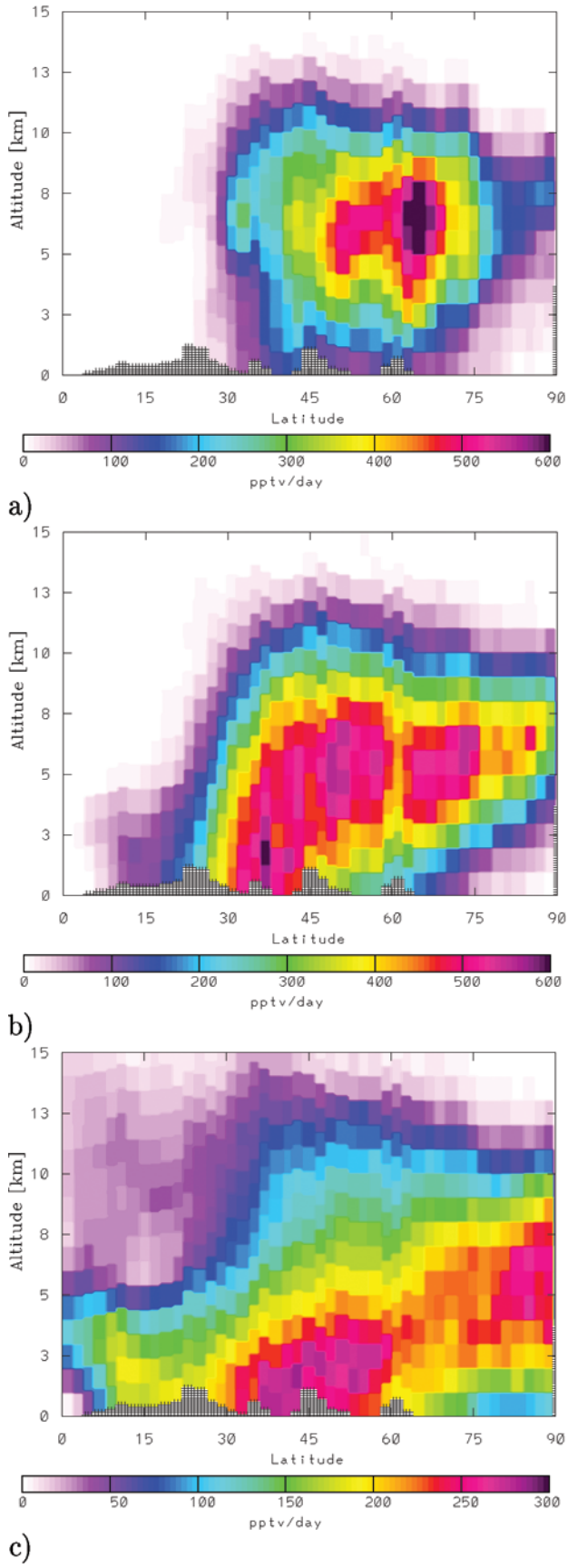


[26] Due to space limitations, an equally detailed description is impossible for the other tracers. We recommend viewing the image loops available on our Internet website and show only the summary panels in the following. In terms of vertical transport the North America tracer (Figure 7) behaves intermediately between the Asia and Europe tracers. Zonal transport is fast in the extratropical NH, but little tracer reaches the SH. Meridional transport is characterized by the fastest eastward movement of all NH tracers. Only a minor fraction of North America tracer, mostly from Mexico, is exported to the Pacific. However, this tracer can loop around the subtropical anticyclone located over the eastern Pacific and return to North America at higher latitudes. In measurement data such recirculated pollution may be confused easily with ICT from Asia.

[27] Africa tracer (Figure 8) experiences strong vertical transport. For Africa as a whole there are small seasonal differences as the ITCZ moves back and forth across Africa. Differences become apparent only if emissions for northern and southern Africa are viewed separately. Because Africa is bounded on both sides by the subtropical transport barriers, Africa tracer is largely confined to the tropics. Most of it tracks slowly across the Atlantic Ocean, reaching the Americas after 25–30 days. But, depending on the season, emissions from the northernmost and southernmost tips of Africa can be injected into the midlatitude stormtracks. Emissions from South Africa can at times cross the Indian Ocean and reach Australia after only a few days.

[28] South America tracer (Figure 9) experiences rapid lifting during the first few days and is equally distributed throughout the entire depth of the troposphere after only 6–8 days. Like for Africa tracer meridional transport is quite slow, but more South America tracer is transported to the south pole, especially in JJA, when the stormtrack shifts equatorward. Zonal transport is faster than for the Africa tracer. Most of the tracer initially tracks toward the Pacific, but emissions from the southern end of the continent can also be advected into the Atlantic and can reach southern Africa after only 4 days.

[29] Compared with NH continents, Australia is located at rather low latitudes. Nevertheless Australia tracer (Figure 10), like Europe tracer, spreads relatively slow into the vertical. Much of it is transported relatively fast toward the south pole, where at 15–20 days its concentrations are comparable to or exceeding those of the Africa and South America tracers, even though Australia's emissions are much lower. Zonal transport is fast and mostly toward the east.

[30] Figure 11 compares the average height in the atmosphere of the six tracers in dependence of their age. Typically the tracers spread vertically relatively fast during the first 5–10 days, after which additional vertical expansion is slow. Factors determining the initially rapid lifting are boundary layer turbulence, deep convection, transport over mountain ranges, and transport with WCBs. After about 5–10 days, these processes become inefficient, because at this

**Figure 13.** (opposite) Altitude-latitude sections of the North America tracer at 5°E for ages of a) 4–6 days, b) 10–12 days, and c) 20–25 days, during MAM. The hatched area indicates the height of the topography.

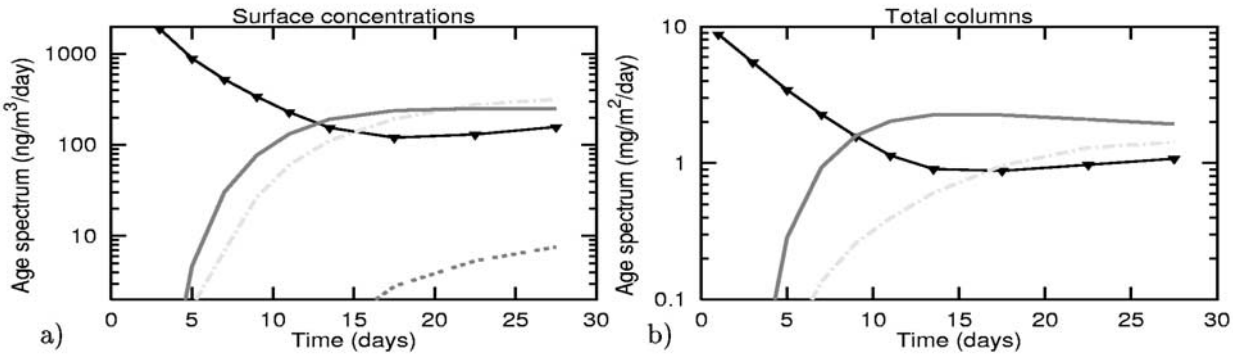


**Figure 14.** Annual average age spectra of the surface concentrations (a) and the total columns (d) of the six tracers in the North America box in dependence of the tracer age. The linestyles are as in Figure 11: North America tracer (solid black line with triangles), Europe tracer (dash-dotted grey line), Asia tracer (thick dark grey line), South America tracer (dashed black line), Africa tracer (thick dotted grey line), Australia (solid black line).

stage the tracer is locally uniformly distributed throughout the entire depth of the troposphere. Further vertical expansion requires transport toward regions with higher tropopause, particularly at low latitudes. However, meridional transport through the subtropics is inefficient [*Yang and Pierrehumbert*, 1994]. Most striking is the contrast between the rapid transport to high altitudes of the Asia tracer and the tendency of the Europe tracer to stay at relatively low levels, particularly in DJF.

## 5. Quantification of ICT

[31] It is a general feature of ICT that tracer signals from an upwind continent first arrive in the upper troposphere, because transport is fastest there. This is seen in Figure 12, which shows cross-sections of the Asia tracer at the North American west coast (125°W) during spring for different age classes. Little tracer arrives during the first four days, but for age class 3 (4–6 days) a clear signal is found at about 10 km altitude (Figure 12a). This is tracer that was lifted by convection or WCBs soon after its release, and subsequently traveled with the jet stream. At 8–10 days (Figure 12b), the maximum signal has descended to 6–8 km, and tracer is seen at the surface, too. For age class 9 (20–25 days) (Figure 12c), the tracer maximum has subsided to the surface and is found further south than the fresher tracer. While, at this age, Asia tracer could have crossed the Pacific with the slow surface winds, it is more consistent with previous findings (e.g., Figure 11) that most of it was transported at higher altitudes and got trapped in the quasi-permanent subtropical anticyclone west of North America, where it subsided.

[32] It has been noted that pollutants from North America are hardly ever seen at the surface in Europe [e.g., *Derwent et al.*, 1998]. Figure 13, cross-sections of the North America tracer at 5°E for different age classes, explains why. For fresh tracer (e.g., 4–6 days), the concentrations are highest at 5–8 km, and north of 60°N (Figure 13a). At the surface tracer mixing ratios are about an order of magnitude lower and thus a North American signal is difficult to detect. For age class 6 (10–12 days) (Figure 13b), the North American plume is centered at a few kilometers altitude. The tracer extends down to the surface, but only south of the Pyrenees and Alps, where few measurement stations are located. At 20–25 days (Figure 13c), the tracer maximum is located right over the Mediterranean at about 40° latitude. Some

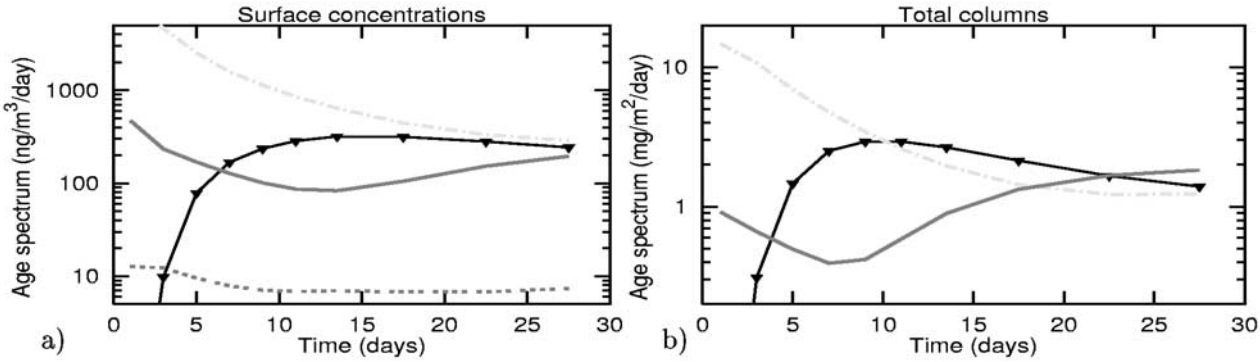


**Figure 15.** Same as Figure 14, but for the Europe box.

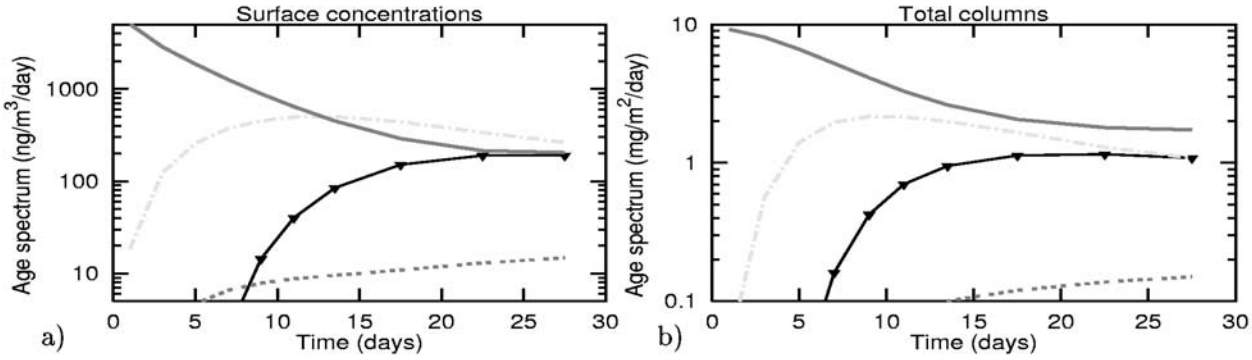


**Figure 16.** Same as Figure 14, but for the Asia box.

tracer is also found further north but at this age attributing a measured substance to a North American source is tricky, because of mixing with fresher European emissions and because it is difficult to describe the transport over such long time intervals accurately enough on a case-study basis. Southward and downward transport of the North America tracer into the Mediterranean is found during the whole year and throughout the Mediterranean. Downward mixing over the mountain ranges of the Alps and Pyrenees is important for this, with processes similar to those reported for North America [*Hacker et al.*, 2001], but trapping and descent in the Azores' high certainly also is key. Aged Asia tracer has a surface maximum at the same location, too. Note that the Mediterranean is the region in Europe with the highest $O_3$ concentrations, where often multiple pollution layers are found aloft [*Millán et al.*, 1997].

[33] Next we quantify the contribution of each tracer to the total tracer burden over every continent and over the Arctic. For this, we defined 7 receptor boxes, as shown in Figure 1. We determined both surface concentrations and total columns. Generally the domestic source dominates the surface concentrations during the first few days after emission. Later on, the concentrations of foreign tracers and thus ICT, can exceed the domestic source. The decomposition of the tracers into age spectra may appear somewhat artificial in this respect, as aged foreign tracers can be mixed with fresh domestic tracer, and, depending on the lifetime of a species, the domestic source may therefore dominate the total burden most of the time, but it supports our understanding.

[34] Over North America the domestic tracer dominates surface concentrations during the first 10–15 days (Figure 14a), depending on the season. Later the Asia tracer makes the largest contribution, and for tracer older than 20 days, Europe becomes equally important. For the total tracer columns (Figure 14b), the domestic tracer is less important, and Asia tracer starts to exceed it already at 6–10 days.

[35] At the European surface (Figure 15a), the domestic tracer exceeds the others for all age classes throughout the year, with the exception of JJA when vertical transport is stronger. Asia tracer ranks second for young ages, due to sporadic westward transport events. However, as these events normally do not penetrate deep into Europe, Asia tracer concentrations decrease with age, and after about 6 days the North America tracer is more important. For the total columns (Figure 15b), the North America tracer exceeds the European contribution after about 8–10 days.

[36] In the Asia box (Figure 16) the domestic source clearly dominates the total columns for all age classes, but at the surface it is exceeded by the Europe tracer after about 10–15 days. This is just the opposite of the Europe box, where the domestic tracer dominates at the surface but not for the total columns. It demonstrates how differences in vertical transport between the Asia and the Europe tracer affect ICT budgets. The strong contribution of European CO

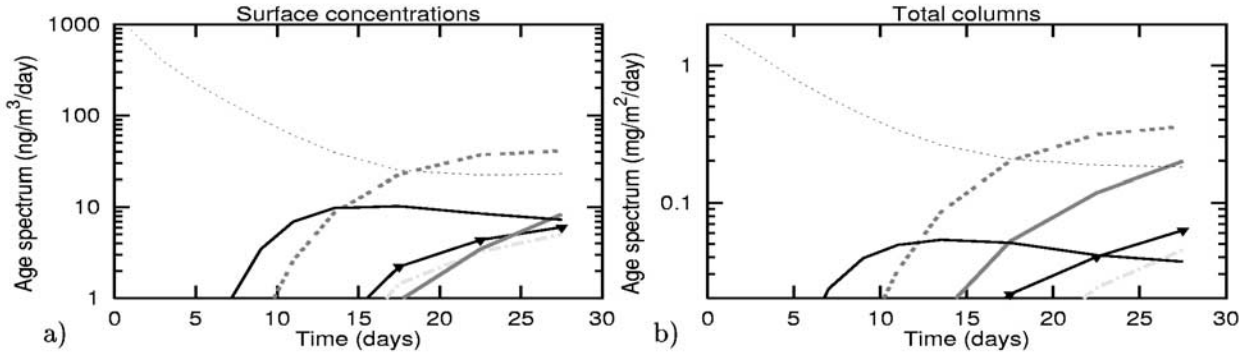


**Figure 17.** Same as Figure 14, but for the South America box.

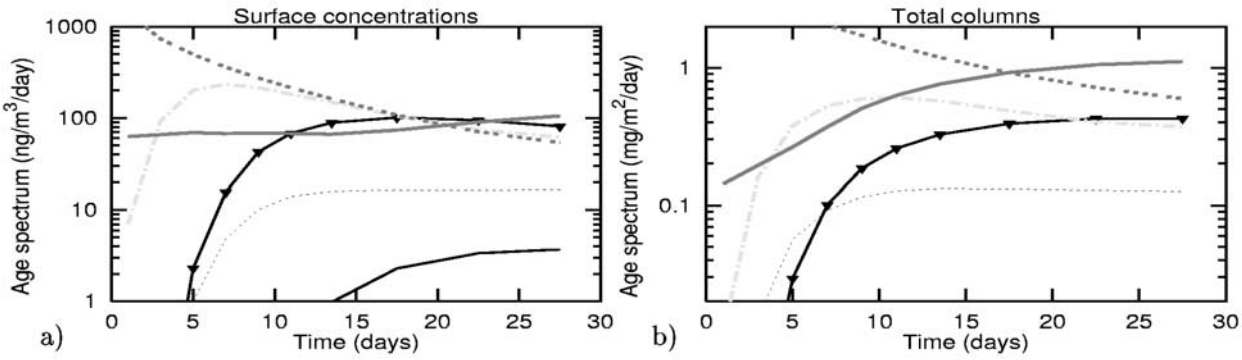


**Figure 18.** Same as Figure 14, but for the Africa box.

at the surface and at higher latitudes of Asia was also found in a recent chemistry model study by *Bey et al.* [2001].

[37] Over South America (Figure 17) domestic tracer exceeds the others both at the surface and for the total columns during the first 15–20 days. This is longer than over all other continents, due to the isolated location of South America. In the Africa box (Figure 18), domestic emissions dominate during the first 10 days (at the surface) to 15–20 days (for the columns). At the surface, Europe, North America and Asia tracers are all of about the same magnitude as the domestic tracer at later times. South America tracer makes a surprisingly small contribution, because most of it travels westward with the slow tropical circulation and does not reach Africa within 30 days. Australia (Figure 19) is the only continent where the domestic tracer is almost negligible, except for the very first days.

[38] In the Arctic (Figure 20), the contribution from the three NH continents is almost constant with age, except for the first few days. Europe tracer exceeds the others, both for the total columns and, even more so, at the surface. This is most pronounced in winter, and is enhanced close to the pole. Thus, European emissions appear to be primarily responsible for causing the Arctic haze problem.

[39] It is clear that ICT depends strongly on the lifetime of a substance. In Tables 1–4 we report the relative contributions of the 6 tracers to the total tracer columns in the 7 receptor boxes for assumed e-folding tracer lifetimes of 2, 5, 10, and 20 days. These contributions were derived from the discrete age spectra and are thus of limited accuracy, but still give an idea of the strong differences between shorter- and longer-lived species, respectively. Note that for a lifetime of 20 days the impact of ICT is underestimated, due to the truncation of the age spectra at 30 days. Note also that at the surface domestic sources make a larger contribution than reported below, whereas in the upper troposphere the opposite is the case.

[40] For a tracer lifetime of 2 days (Table 1) the domestic source generally dominates. Over North and South America foreign tracers contribute less than 1% to the total tracer mass, because upwind continents are far away. Over Australia, which has the smallest domestic emissions, import from Asia and Africa together account for 20% of the total mass. Over the Arctic, Europe tracer contributes 83% of the tracer mass.

[41] Given a tracer lifetime of 5 days (Table 2), we see that foreign sources become important over all continents, with the exception of South America, where the domestic source still contributes 96%. Over Australia, in contrast, the domestic source makes up only 23%, whereas import from Asia accounts for almost half of the tracer. Over the NH continents, domestic sources are still most important, but approximately a third of the tracer mass is contributed by the upwind continent.

[42] For a tracer lifetime of 10 days (Table 3), import from more than one foreign continent becomes important. For instance, North America receives 46% and 8% from

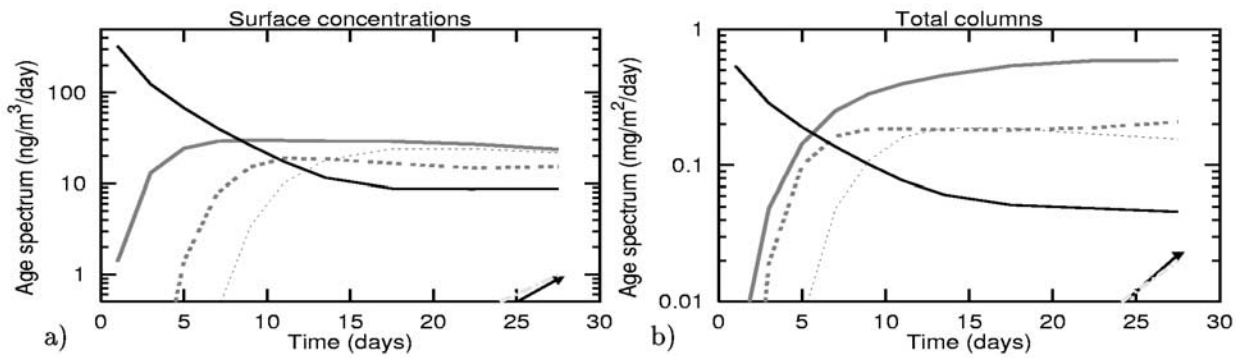


**Figure 19.** Same as Figure 14, but for the Australia box.

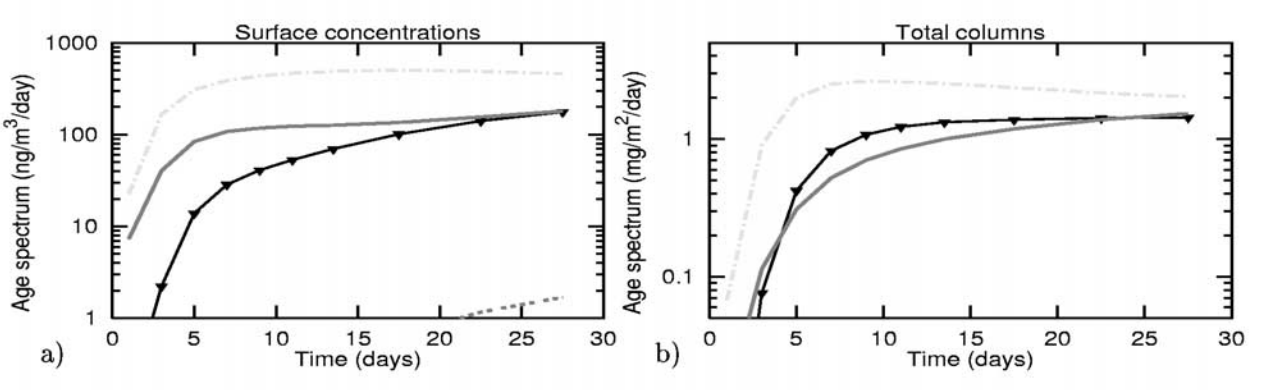


**Figure 20.** Same as Figure 14, but for the Arctic box.

Asia and Europe, respectively. Africa receives significant import from all other continents, except for Australia.

[43] For a tracer lifetime of 20 days (Table 4), foreign sources can become more important than the domestic source. North America receives 57% of the tracer mass from Asia, Europe receives 47% from North America, and Asia receives 34% from Europe. Europe tracer still dominates over the Arctic, but Asia and North America tracers are more important than for shorter-lived species. Because old tracer is mixed rather well within a hemisphere, the relative contributions of the different tracers tend to approach the relative source strengths of the different continents. For long-lived species, e.g., most of the greenhouse gases, the details of ICT therefore become unimportant.

## 6. Conclusions

[44] This paper presented results of a simulation of tracer transport during the year 2000. Six tracers were released over the continents according to an emission inventory for CO, and Lagrangian concepts were used to derive age spectra of the tracer concentrations on a global grid in order to establish the timescales and pathways of pollution export from the continents. An Internet webpage was created where movies of both the horizontal and vertical transport of the tracers can be viewed. The following conclusions can be drawn:

1. Asia tracer experiences the fastest vertical transport of all tracers. On timescales of a few days it is distributed throughout the entire depth of the troposphere. This is valid both for emissions into the midlatitude stormtrack, where WCBs are responsible for the upward transport, and emissions injected into the summer monsoon flow. Emissions into the winter monsoon flow are at first confined beneath the trade wind inversion, but are also rapidly lifted once they reach the ITCZ.

2. Europe tracer has a strong tendency to remain in the lower troposphere, because Europe is located at higher latitudes than the other continents and at the end rather than at the beginning of a stormtrack. Europe tracer accumulates in the Arctic, especially in DJF. European emissions thus seem to be the main cause of the Arctic haze problem.

3. All other tracers behave intermediately between Asia and Europe tracer in terms of vertical transport. North America tracer features the fastest meridional export of all tracers, with the plume center being located over the Atlantic Ocean at 6–8 days. Africa tracer is the one with the weakest meridional mixing, because Africa is confined on both sides by subtropical transport barriers. A large fraction of Australia's emissions is transported toward the Antarctic.

4. It is a general feature of ICT that tracer signals from an upwind continent first arrive in the upper troposphere, typically after some 4 days. After travel times of about 10 days, tracer also arrives in the lower troposphere, but not at the same location as the upper tropospheric signal. In the extratropics the maximum impact at the surface is shifted toward lower latitudes relative to the upper tropospheric signal.

**Table 1.** Relative Contribution[a] of the Six Emission Tracers to the Total Tracer Columns in the Seven Receptor Boxes for a Tracer Lifetime of 2 Days

| Receptors | North America | Europe | Asia | South America | Africa | Australia |
|---|---|---|---|---|---|---|
| North America | 99.6 | 0.1 | 0.3 | 0.0 | 0.0 | 0.0 |
| Europe | 2.6 | 91.2 | 5.6 | 0.0 | 0.5 | 0.0 |
| Asia | 0.0 | 6.5 | 93.4 | 0.0 | 0.1 | 0.0 |
| South America | 0.0 | 0.0 | 0.0 | 100.0 | 0.0 | 0.0 |
| Africa | 0.1 | 4.9 | 6.0 | 0.5 | 88.6 | 0.0 |
| Australia | 0.0 | 0.0 | 13.7 | 0.0 | 5.4 | 80.9 |
| Arctic | 7.0 | 82.6 | 10.4 | 0.0 | 0.0 | 0.0 |

[a]Relative contribution is expressed in %.

**Table 2.** Relative Contribution[a] of the Six Emission Tracers to the Total Tracer Columns in the Seven Receptor Boxes for a Tracer Lifetime of 5 Days

| Receptors | North America | Europe | Asia | South America | Africa | Australia |
|---|---|---|---|---|---|---|
| North America | 67.9 | 4.0 | 27.9 | 0.2 | 0.0 | 0.0 |
| Europe | 32.5 | 61.7 | 5.1 | 0.0 | 0.7 | 0.0 |
| Asia | 2.2 | 26.6 | 70.6 | 0.0 | 0.7 | 0.0 |
| South America | 0.1 | 0.0 | 0.0 | 95.7 | 0.3 | 3.9 |
| Africa | 3.2 | 16.7 | 11.8 | 2.9 | 65.3 | 0.0 |
| Australia | 0.0 | 0.0 | 41.9 | 8.1 | 27.2 | 22.8 |
| Arctic | 21.3 | 65.1 | 13.6 | 0.0 | 0.1 | 0.0 |

[a]Relative contribution is expressed in %.

**Table 3.** Relative Contribution[a] of the Six Emission Tracers to the Total Tracer Columns in the Seven Receptor Boxes for a Tracer Lifetime of 10 Days

| Receptors | North America | Europe | Asia | South America | Africa | Australia |
|---|---|---|---|---|---|---|
| North America | 45.7 | 7.6 | 46.3 | 0.3 | 0.1 | 0.0 |
| Europe | 42.8 | 50.3 | 6.1 | 0.0 | 0.8 | 0.0 |
| Asia | 6.3 | 31.9 | 60.8 | 0.0 | 1.0 | 0.0 |
| South America | 0.4 | 0.0 | 0.1 | 89.4 | 2.0 | 8.1 |
| Africa | 5.9 | 19.0 | 16.2 | 3.7 | 55.1 | 0.0 |
| Australia | 0.0 | 0.0 | 46.0 | 14.9 | 25.3 | 13.9 |
| Arctic | 24.5 | 59.5 | 16.0 | 0.0 | 0.1 | 0.0 |

[a]Relative contribution is expressed in %.

5. Foreign tracers contribute a larger fraction to the total tracer burden in the upper than in the lower troposphere, whereas domestic tracers are relatively more important at the surface.

6. Assuming a 2-day lifetime of the tracers, the domestic tracers dominate total tracer columns over all continents. Only over Australia foreign tracers account for 20% of the tracer mass. This changes for longer tracer lifetimes. For instance, for a 20-day lifetime North America receives 57% of the tracer burden from Asia and 11% from Europe, Europe receives 47% from North America and 9% from Asia, and Asia receives 34% from Europe and 11% from North America. Over Australia, the domestic tracer accounts for less than 10%.

[45] Three regions of special interest have been identified, which are recommended for further exploration by deploying future field campaigns:

1. In DJF Asia tracer accumulates over Indonesia and the Indian Ocean. This region and time of year is speculated to be a stratospheric fountain [*Newell and Gould-Stewart*, 1981], where most of the tropospheric air enters the stratosphere. It is thus probable that pollutants emitted in Asia can be transferred directly into the stratosphere with only moderate previous dilution in the troposphere.

2. In JJA the highest concentrations of the Asia tracer are found in the Middle East. After ascending in the monsoon flow and traveling westward at about 200 hPa, the tracer gets trapped in the subtropical high over the Middle East and descends there, presumably mixing with domestic emissions. *Li et al.* [2001b] have identified this region as the one with the highest simulated $O_3$ concentrations worldwide in their model.

**Table 4.** Relative Contribution[a] of the Six Emission Tracers to the Total Tracer Columns in the Seven Receptor Boxes for a Tracer Lifetime of 20 Days

| Receptors | North America | Europe | Asia | South America | Africa | Australia |
|---|---|---|---|---|---|---|
| North America | 31.9 | 11.0 | 56.6 | 0.3 | 0.1 | 0.0 |
| Europe | 47.4 | 42.1 | 9.5 | 0.1 | 1.0 | 0.0 |
| Asia | 11.2 | 34.5 | 52.9 | 0.0 | 1.4 | 0.0 |
| South America | 0.9 | 0.0 | 0.8 | 79.2 | 7.5 | 11.5 |
| Africa | 8.4 | 19.7 | 20.6 | 4.2 | 47.1 | 0.0 |
| Australia | 0.0 | 0.0 | 48.4 | 19.5 | 22.6 | 9.4 |
| Arctic | 26.2 | 55.6 | 18.1 | 0.0 | 0.1 | 0.0 |

[a]Relative contribution is expressed in %.

3. In JJA North America tracer arrives over northwestern Europe in the middle and upper troposphere, but descends (also partly because of downward mixing over mountain ranges) as it travels southwards into the subtropical high. The highest surface concentrations of the North America tracer over Europe are therefore found in the Mediterranean, the region with the highest $O_3$ concentrations in Europe and a strong layering of the $O_3$ [*Millán et al.*, 1997]. Attribution of plumes to a North American origin may be difficult there, though, because of the high tracer age.

[46] The year 2000 was in the cold El Niño/Southern Oscillation phase and had positive values of the North Atlantic Oscillation (NAO) index at the beginning and negative ones at the end. WCBs in the North Atlantic shift toward the north for positive NAO (Eckhardt, unpublished results), and thus more than normal North American emissions may have been transported to the upper troposphere and to Europe at the beginning of the simulation, but less at the end. Global circulation patterns were at least not particularly unusual and the main transport patterns found in this study should be representative also for other years. Interannual variations of ICT are likely to occur with circulation anomalies, but their quantification remains a task for future studies.

[47] **Acknowledgments.** This study was part of the projects CARLOTTA, ATMOFAST and CONTRACE, funded by the German Federal Ministry for Education and Research within the Atmospheric Research Program 2000. K. Emanuel is acknowledged for providing the source code of his convection scheme, and P. Seibert for implementing it into FLEXPART. ECMWF and the German Weather Service are acknowledged for permitting access to the ECMWF archives. Part of this study was done while AS was guest at the NOAA Aeronomy Laboratory (AL). AS thanks the AL staff for their hospitality, and particularly O. Cooper and M. Trainer for enlightening discussions.

## References

Andreae, M. O., et al., Vertical distribution of dimethylsulfide, sulfur dioxide, aerosol ions, and radon over the North-East Pacific Ocean, *J. Atmos. Chem.*, *6*, 149–173, 1988.

Bailey, R., L. A. Barrie, C. J. Halsall, P. Fellin, and D. C. G. Muir, Atmospheric organochlorine pesticides in the western Canadian arctic: Evidence of transpacific transport, *J. Geophys. Res.*, *105*, 11,805–11,811, 2000.

Barrie, L. A., Arctic air pollution: An overview of current knowledge, *Atmos. Environ.*, *20*, 643–663, 1986.

Berntsen, T. K., S. Karlsdottir, and D. A. Jaffe, Influence of Asian emissions on the composition of air reaching the North Western United States, *Geophys. Res. Lett.*, *26*, 22,171–22,174, 1999.

Bey, I., D. J. Jacob, J. A. Logan, and R. M. Yantosca, Asian chemical outflow to the Pacific in spring: Origins, pathways, and budgets, *J. Geophys. Res.*, *106*, 23,097–23,113, 2001.

Cooper, O. R., et al., Trace gas signatures of the airstreams within North Atlantic cyclones: Case studies from the North Atlantic Regional Experiment (NARE '97) aircraft intensive, *J. Geophys. Res.*, *106*, 5437–5456, 2001.

Derwent, R. G., P. G. Simmonds, S. Seuring, and C. Dimmer, Observation and interpretation of the seasonal cycles in the surface concentrations of ozone and carbon monoxide at Mace Head, Ireland from 1990 to 1994, *Atmos. Environ.*, *32*, 145–157, 1998.

ECMWF, *User Guide to ECMWF Products 2.1*, *Meteorol. Bull. M3.2*, ECMWF, Reading, UK, 1995.

Emanuel, K. A., and M. Zivkovic-Rothman, Development and evaluation of a convection scheme for use in climate models, *J. Atmos. Sci.*, *56*, 1766–1782, 1999.

Fishman, J., K. Fakhruzzaman, B. Croes, and D. Ngana, Identification of widespread pollution in the Southern Hemisphere deduced from satellite analyses, *Science*, *252*, 1693–1696, 1991.

Forster, C., et al., Transport of forest fire emissions from Canada to Europe, *J. Geophys. Res.*, *106*, 22,887–22,906, 2001.

Garstang, M., et al., Horizontal and vertical transport of air over southern Africa, *J. Geophys. Res.*, *101*, 23,721–23,736, 1996.

Hacker, J. P., I. G. McKendry, and R. B. Stull, Modeled downward transport of a passive tracer over western North America during an Asian dust event in April 1998, *J. Appl. Meteorol.*, *40*, 1617–1628, 2001.

Hamelin, B., F. E. Grousset, P. E. Biscaye, A. Zindler, and J. M. Prospero, Lead isotopes in trade wind aerosols at Barbados: The influence of European emissions over the North Atlantic, *J. Geophys. Res.*, *94*, 16,243–16,250, 1989.

Husar, R. B., et al., Asian dust events of April 1998, *J. Geophys. Res.*, *106*, 18,317–18,330, 2001.

Jacob, D. J., J. A. Logan, and P. P. Murti, Effect of rising Asian emissions on surface ozone in the United States, *Geophys. Res. Lett.*, *26*, 2175–2178, 1999.

Jaeschke, W., et al., Measurements of trace substances in the Arctic troposphere as potential precursors and constituents of Arctic haze, *J. Atmos. Chem.*, *34*, 291–319, 1999.

Jaffe, D., et al., Transport of Asian air pollution to North America, *Geophys. Res. Lett.*, *26*, 711–714, 1999.

Jennings, S. G., T. G. Spain, B. G. Doddridge, H. Maring, B. P. Kelly, and A. D. A. Hansen, Concurrent measurements of black carbon aerosol and carbon monoxide at Mace Head, *J. Geophys. Res.*, *101*, 19,447–19,454, 1996.

Lelieveld, J., et al., The Indian Ocean Experiment: Widespread air pollution from South and Southeast Asia, *Science*, *291*, 1031–1036, 2001.

Li, Q., et al., Sources of ozone over the North Atlantic and trans-Atlantic transport of pollution: A global model perspective, *IGACt. Newsl.*, *24*, 12–17, 2001a.

Li, Q., et al., A tropospheric ozone maximum over the Middle East, *Geophys. Res. Lett.*, *28*, 3235–3238, 2001b.

Lu, J. Y., et al., Magnification of atmospheric mercury deposition to polar regions in springtime: The link to tropospheric ozone depletion chemistry, *Geophys. Res. Lett.*, *28*, 3219–3222, 2001.

Millán, M., R. Salvador, E. Mantilla, and G. Kallos, Photo-oxidant dynamics in the Mediterranean basin in summer: Results from European research projects, *J. Geophys. Res.*, *102*, 8811–8823, 1997.

Newell, R. E., and M. J. Evans, Seasonal changes in pollutant transport to the North Pacific: The relative importance of Asian and European sources, *Geophys. Res. Lett.*, *27*, 2509–2512, 2000.

Newell, R. E., and S. Gould-Stewart, A stratospheric fountain?, *J. Atmos. Sci.*, *51*, 2789–2796, 1981.

Olivier, J. G. J., et al., Description of EDGAR Version 2.0. A set of global emission inventories of greenhouse gases and ozone depleting substances for all anthropogenic and most natural sources per country basis and on $1 \times 1$ grid, RIVM Rep. No. 771060 002 [TNO MEP Rep. No. R96/119], December 1996, RIVM Bilthoven, 1996.

Parrish, D. D., et al., Indications of photochemical histories of Pacific air masses from measurements of atmospheric trace species at Pt. Arena, California, *J. Geophys. Res.*, *97*, 15,883–15,901, 1992.

Parrish, D. D., M. Trainer, J. S. Holloway, J. E. Yee, M. S. Warshawsky, F. C. Fehsenfeld, G. L. Forbes, and J. L. Moody, Relationships between ozone and carbon monoxide at surface sites in the North Atlantic region, *J. Geophys. Res.*, *103*, 13,357–13,376, 1998.

Peixoto, J. P., and A. H. Oort, *Physics of Climate*, American Institute of Physics, New York, 1992.

Prospero, J. M., Long-term measurements of the transport of African mineral dust to the southeastern United States: Implications for regional air quality, *J. Geophys. Res.*, *104*, 15,917–15,927, 1999.

Reiff, J., G. S. Forbes, F. T. M. Spieksma, and J. J. Reynders, African dust reaching northwestern Europe: A case study to verify trajectory calculations, *J. Clim. Appl. Meteorol.*, *25*, 1543–1567, 1986.

Schmitt, R., Simultaneous measurements of carbon monoxide, ozone, PAN, NMHC and aerosols in the free troposphere at Izaña, Canary Islands, in *Proceedings of the EUROTRAC Symposium '94*, edited by P. M. Borrell, pp. 313–316, SPB Academic, The Hague, Netherlands, 1994.

Schultz, M., R. Schmitt, K. Thomas, and A. Volz-Thomas, Photochemical box modeling of long-range transport from North America to Tenerife during the North Atlantic Regional Experiment (NARE) 1993, *J. Geophys. Res.*, *103*, 13,477–13,488, 1998.

Seibert, P., B. Krüger, and A. Frank, Parametrisation of convective mixing in a Lagrangian particle dispersion model, in *Proceedings of the 5th GLOREAM Workshop, Wengen, Switzerland*, 24–26 September, 2001.

Spichtinger, N., M. Wenig, P. James, T. Wagner, U. Platt, and A. Stohl, Satellite detection of a continental-scale plume of nitrogen oxides from boreal forest fires, *Geophys. Res. Lett.*, *28*, 4579–4582, 2001.

Stohl, A., A one-year Lagrangian "climatology" of airstreams in the northern hemisphere troposphere and lowermost stratosphere, *J. Geophys. Res.*, *106*, 7263–7279, 2001.

Stohl, A., and D. J. Thomson, A density correction for Lagrangian particle dispersion models, *Boundary Layer Meteorol.*, *90*, 155–167, 1999.

Stohl, A., and T. Trickl, A textbook example of long-range transport: Simultaneous observation of ozone maxima of stratospheric and North American origin in the free troposphere over Europe, *J. Geophys. Res.*, *104*, 30,445–30,462, 1999.

Stohl, A., and T. Trickl, Experimental evidence for trans-Atlantic transport of air pollution, *IGACt. Newsl.*, *24*, 10–12, 2001.

Stohl, A., M. Hittenberger, and G. Wotawa, Validation of the Lagrangian particle dispersion model FLEXPART against large scale tracer experiment data, *Atmos. Environ.*, *24*, 4245–4264, 1998.

Stohl, A., et al., The influence of stratospheric intrusions on alpine ozone concentrations, *Atmos. Environ.*, *34*, 1323–1354, 2000.

Stohl, A., M. Trainer, T. Ryerson, J. Holloway, and D. Parrish, Export of $NO_y$ from the North American boundary layer during 1996 and 1997 North Atlantic Regional Experiments, *J. Geophys. Res.*, *107*, 4131, doi:10.1029/2001JD000519, 2002.

Sturman, A. P., P. D. Tyson, and P. C. D'Abreton, A preliminary study of the transport of air from Africa and Australia to New Zealand, *J. R. Soc. N. Z.*, *27*, 485–498, 1997.

Swap, R., S. Ulanski, M. Cobbett, and M. Garstang, Temporal and spatial characteristics of Saharan dust outbreaks, *J. Geophys. Res.*, *101*, 4205–4220, 1996.

Thompson, A. M., et al., Where did tropospheric ozone over southern Africa and the tropical Atlantic come from in October 1992? Insights from TOMS, GTE TRACE A, and SAFARI 1992, *J. Geophys. Res.*, *101*, 24,251–24,278, 1996.

Tyson, P. D., and P. C. D'Abreton, Transport and recirculation of aerosols off Southern Africa—macroscale plume structure, *Atmos. Environ.*, *32*, 1511–1524, 1998.

Wenig, , et al., Transport of power plant emissions from South Africa to Australia, *Nature*, manuscript in preparation, 2002.

Wild, O., and H. Akimoto, Intercontinental transport of ozone and its precursors in a three-dimensional global CTM, *J. Geophys. Res.*, *106*, 27,729–27,744, 2001.

Wild, O., K. S. Law, K. S. McKenna, B. J. Bandy, S. A. Penkett, and J. Pyle, Photochemical trajectory modeling studies of the North Atlantic region during August 1993, *J. Geophys. Res.*, *101*, 29,269–29,288, 1996.

Wilkening, K. E., L. A. Barrie, and M. Engle, Trans-Pacific air pollution, *Science*, *290*, 65–67, 2000.

Yang, H., and R. T. Pierrehumbert, Production of dry air by isentropic mixing, *J. Atmos. Sci.*, *51*, 3437–3454, 1994.

Yienger, J. J., et al., The episodic nature of air pollution transport from Asia to North America, *J. Geophys. Res.*, *105*, 26,931–26,945, 2000.

S. Eckhardt, C. Forster, P. James, N. Spichtinger, and A. Stohl, Lehrstuhl für Bioklimatologie und Immissionsforschung, Technische Universität München, Am Hochanger 13, D-85354 Freising-Weihenstephan, Germany. (as@tracy.fw.tum.de)